



# Electronic and elastic properties cubic of $\text{LiBH}_4$ and $\text{Li}(\text{BH})_3$ as host materials for hydrogen storage

Osman Örne<sup>1</sup>, Selgin Al<sup>2,a</sup> , Ahmet İyigor<sup>3</sup>, and Süleyman Lafci<sup>4</sup>

<sup>1</sup> Department of Metallurgy and Material Engineering, Kırşehir Ahi Evran University, Kırşehir, Turkey

<sup>2</sup> Department of Environmental Protection Technologies, Izmir Democracy University, Izmir, Turkey

<sup>3</sup> Department of Machine and Metal Technologies, Kırşehir Ahi Evran University, Kırşehir, Turkey

<sup>4</sup> Institute of Science, Kırşehir Ahi Evran University, Kırşehir, Turkey

Received 19 August 2023 / Accepted 9 January 2024 / Published online 20 January 2024  
© The Author(s), under exclusive licence to EDP Sciences, SIF and Springer-Verlag GmbH Germany, part of Springer Nature 2024

**Abstract.** Due to growing interest to explore and predict potential hydrogen storage materials by adopting theoretical and greatly functional software, research on lightweight materials has taken great attention. From this perspective, this study focuses on investigating electronic, elastic, and anisotropic properties of cubic  $\text{LiBH}_4$  and  $\text{Li}(\text{BH})_3$  using first principles calculations for the first time. A comprehensive investigation has been carried out to reveal materials' electronic, elastic, hardness, and anisotropic behaviour. The calculations exhibit that both  $\text{LiBH}_4$  and  $\text{Li}(\text{BH})_3$  has negative formation energies as  $-0.268$  eV/atom and  $-0.187$  eV/atom, respectively which indicate synthesizability and thermodynamic stability. Elastic constants of materials are used to predict mechanical stabilities based on the well-known Born stability criteria. It is seen that both materials are mechanically stable. The electronic band structures indicate band gaps between valence and conduction band as 6 eV for  $\text{LiBH}_4$  and 4.58 eV for  $\text{Li}(\text{BH})_3$ , showing non-metallic nature of both materials. The negative Cauchy pressures and the B/G ratio less than 1.75 indicate brittleness of both materials. The anisotropy factors of both materials display that these materials are anisotropic due to a deviation from unity. The hydrogen desorption temperature is also estimated as  $\sim 198.2$  K for  $\text{LiBH}_4$  and  $\sim 138.6$  K for  $\text{Li}(\text{BH})_3$ .

## 1 Introduction

One promising and logical strategy to mitigate the effects of global warming and pollution is to reduce the use of carbon-based fuels and boost carbon free renewable sources. One way of achieving this aim is to utilise hydrogen in energy demanding sectors. Hydrogen is currently used in chemical industry worldwide; it is crucial to spread its usage for energy sector and transportation. Moreover, the development of modern society requires a great deal of energy in the global scale. In this sense, production of green hydrogen even grey hydrogen can effectively help the cause [1]. However, use of hydrogen as an energy carrier possesses a few steps one of which is storage of it. The main obstacle for widespread use of hydrogen comes from materials related issues for storage. Finding a material that satisfies all the requirements, such as cost, high hydrogenation/dehydrogenation kinetics, safety etc., is a challenge which demands an urgent solution for efficient energy storage while going green globally. Discovery and investigation of novel materials mostly rely on experimental studies which are based on trial bases and require

long time, infrastructure, and expensive lab equipment. With the development of quantum mechanics and high-performance computers, the materials' chemical and physical properties can be explored computationally which is time- and cost-saving. The properties of advanced materials can be computed using high-performance computers which can calculate the interactions between ions and electron in a very short time. Density functional theory (DFT) investigations have been used for this purpose for a couple of decades which is very helpful to build huge materials database such as Materials Project. Using this approach, a huge amount of advanced materials' properties can be explored. From this database, the experimentalists can choose the materials to design their experiments which will save time. From this point of view, we use density functional theory to investigate various properties of  $\text{LiBH}_4$  and  $\text{Li}(\text{BH})_3$  for hydrogen storage purposes.

$\text{LiBH}_4$  has been taking a great deal of attention due to its high gravimetric hydrogen density for solid-state hydrogen storage. The materials have a few space groups, but it comes to our attention that some of these space groups have not been studied previously.

<sup>a</sup> e-mail: [selgin.al@idu.edu.tr](mailto:selgin.al@idu.edu.tr) (corresponding author)

The ground state structures of  $\text{LiBH}_4$  have been studied using the DFT and a new stable orthogonal structure with Pnma symmetry was suggested along with orthorhombic and hexagonal structure previously [2]. The elastic properties of orthorhombic Pnma  $\text{LiBH}_4$  along with elastic anisotropy were studied by Li et al. [3] and they reported a mechanically stable, ductile, and elastically anisotropic structure for orthorhombic Pnma  $\text{LiBH}_4$ . In a recent study, the orthorhombic  $\text{LiBH}_4$  has been reported as a brittle and insulating material and the authors' suggested that orthorhombic  $\text{LiBH}_4$  is suitable for hydrogen storage [4]. The elastic and structural properties of orthorhombic  $\text{LiBH}_4$  were also studied by another group using first principles calculations and reported a mechanically stable and brittle structure [5]. The thermodynamic and vibrational properties of orthorhombic and hexagonal  $\text{LiBH}_4$  were studied by Benzidi et al. [6] using ab-initio calculations; it was found that orthorhombic  $\text{LiBH}_4$  is thermodynamically stable, whereas hexagonal  $\text{LiBH}_4$  is unstable due to negative frequency modes. There are also experimental studies to improve hydrogen storage properties of  $\text{LiBH}_4$  by addition of solvents/catalysts and oxides [7, 8]. Unfortunately, there are not much studies exist on  $\text{Li}(\text{BH})_3$  as far as the authors' knowledge. Therefore, this study will contribute to the existing database and evaluate these two materials in terms of hydrogen storage materials. In this paper, first principles investigations have been used to determine electronic, elastic, hardness, and anisotropic properties of cubic  $\text{LiBH}_4$  and  $\text{Li}(\text{BH})_3$ . Several elastic parameters and properties, such as Vickers hardness, anisotropy, and Cauchy pressure, have been computed and examined. The pressure dependence of elastic constants, and bulk and shear modulus have been explored. The electronic band structures and density of states are obtained. Properties of materials have been examined in terms of hydrogen storage.

## 2 Method

Our calculations were conducted using the first principles plane wave pseudopotential method implemented in Quantum Espresso code [9]. The ultra-soft pseudopotentials were adopted to calculate the interaction between the nuclei, valence electron, and the core electrons. The electronic exchange correlation potentials were treated using the generalized slope approximation (GGA) parameterized by Perdew, Burke, and Ernzerhof (PBE) [10]. The cut-offs for wave functions and charge density were evaluated to be 40 Ry and 400 Ry, respectively. Brillouin-zone integrations were performed using Monkhorst–Pack  $12 \times 12 \times 12$  k point grid. It was carried out using the smearing technique [11] with the smearing parameter as  $\sigma = 0.01$  Ry for integration up to the Fermi surface. Elastic properties were computed using the stress–strain method with the help of the thermo-pw program included in the quantum-espresso package program.

## 3 Results and discussion

### 3.1 Structural and mechanical properties

$\text{LiBH}_4$  and  $\text{Li}(\text{BH})_3$  crystallize in the cubic phase with the space groups  $F\bar{4}3m$  (Fig. 1a) and  $Fm\bar{3}m$  (Fig. 1b), respectively, as shown in Fig. 1. The equilibrium lattice constants are calculated and presented in Table 1. First, total energies are calculated as a function of changing unit cell volume around the equilibrium volume where energy-volume data are obtained and presented in Fig. 2. Then, these data are fitted the Murnaghan's equation of state. The equilibrium volume is determined by finding the minimum energy level where the volume is called optimised equilibrium volume, and the energy is called ground state energy.

The computed lattice constants of materials along with formation energies are presented in Table 1. The lattice constants agree with the available data. Formation energies of materials are computed as follows [12–14]:

$$\Delta H_{\text{LiBH}_4} = \frac{E_{\text{T}}^{\text{LiBH}_4} - [E_{\text{Li}} + E_{\text{B}} + 4E_{\text{H}}]_{\text{bulk}}}{6} \quad (1)$$

$$\Delta H_{\text{Li}(\text{BH})_3} = \frac{E_{\text{T}}^{\text{Li}(\text{BH})_3} - [2E_{\text{Li}} + 6E_{\text{B}} + 6E_{\text{H}}]_{\text{bulk}}}{14}, \quad (2)$$

where  $E_{\text{T}}$  signifies total energy of the system and  $E_{\text{Li}}$ ,  $E_{\text{B}}$ , and  $E_{\text{H}}$  signify total energies of Li, B and hydrogen in bulk form.

In addition to formation energies, cohesive energies of materials are computed to determine structural stability as follows [13]:

$$E_{\text{coh}}^{\text{LiBH}_4} = \frac{E_{\text{T}}^{\text{LiBH}_4} - [E_{\text{Li}} + E_{\text{B}} + 4E_{\text{H}}]_{\text{isolated}}}{6} \quad (3)$$

$$E_{\text{coh}}^{\text{Li}(\text{BH})_3} = \frac{E_{\text{T}}^{\text{Li}(\text{BH})_3} - [2E_{\text{Li}} + 6E_{\text{B}} + 6E_{\text{H}}]_{\text{isolated}}}{14}, \quad (4)$$

where  $E_{\text{T}}$  signifies total energy of the system and  $E_{\text{Li}}$ ,  $E_{\text{B}}$ , and  $E_{\text{H}}$  signifies total energy of single isolated atom. Both materials have negative formation energies which indicates synthesizability of the materials and thermodynamic stability. More negative formation energy and higher positive cohesive energy indicate more stability. Positive cohesive energy indicates strong bonding of atoms within the material.  $\text{LiBH}_4$  has more negative formation energy per atom ( $-0.268$  eV/atom) compared to  $\text{Li}(\text{BH})_3$  ( $-0.187$  eV/atom) and more positive cohesive energy ( $2.456$  eV/atom) compared to  $\text{Li}(\text{BH})_3$  ( $2.190$  eV/atom), and thus, it can be predicted that cubic  $\text{LiBH}_4$  is structurally more stable than cubic  $\text{Li}(\text{BH})_3$ .

The calculation of elastic constants has been also carried out and the results are given in Table 1. The elastic constants can allow one to calculate various parameters

**Fig. 1** The crystal structure representatives of  $\text{LiBH}_4$  (a) and  $\text{Li}(\text{BH})_3$  (b)

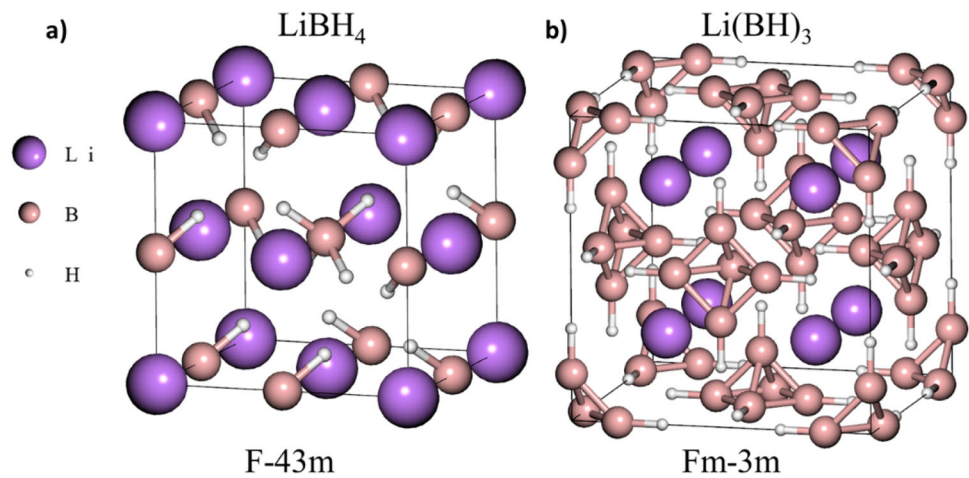


**Table 1** The calculated lattice constants ( $a$ , Å), Formation energies ( $\Delta H_f$ , eV/atom), cohesive energies ( $E_{\text{coh}}$ , eV/atom), and elastic constants ( $C_{11}, C_{12}, C_{44}$ , GPa) of  $\text{LiBH}_4$  and  $\text{Li}(\text{BH})_3$

Material	References	Space group	$a$ (Å)	$\Delta H_f$	$E_{\text{coh}}$	$C_{11}$	$C_{12}$	$C_{44}$
$\text{LiBH}_4$	This work	$F\bar{4}3m$	5.728	- 0.268	2.456	44.75	23.87	26.50
	[2]	$F\bar{4}3m$	5.741					
$\text{Li}(\text{BH})_3$	This work	$Fm\bar{3}m$	7.920	- 0.187	2.190	54.10	9.59	16.30

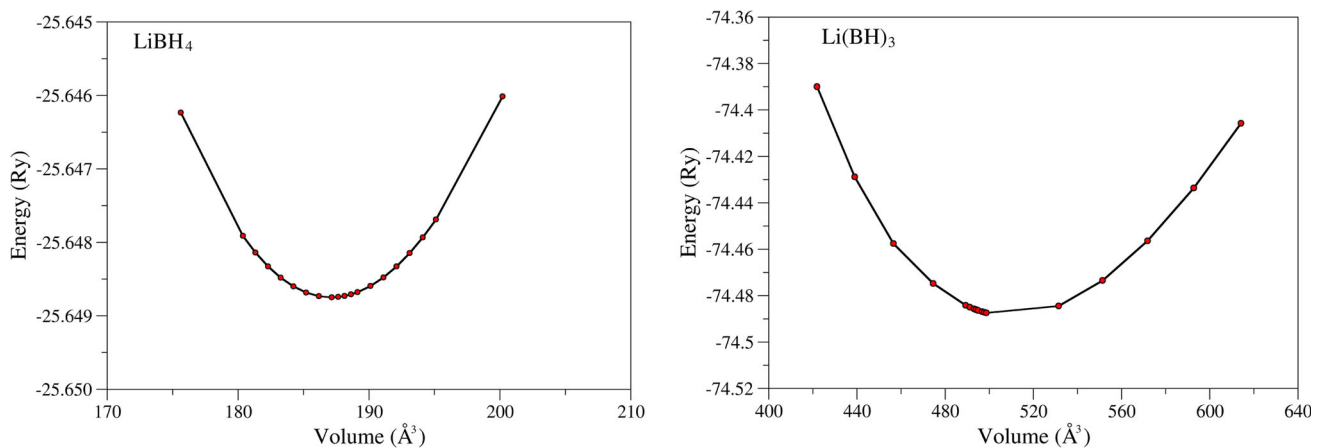


**Fig. 2** Energy versus volume optimisation graphs for  $\text{LiBH}_4$  and  $\text{Li}(\text{BH})_3$

such as Bulk, Shear, and Young modulus which provide information about the materials strength against the external forces. In addition, it can help to understand mechanical stability, interactions of atoms, and bonding. For a cubic structure, there are three independent elastic constants are available as  $C_{11}$ ,  $C_{12}$ , and  $C_{44}$ . The obtained elastic constants take positive value for both materials as seen in Table 1.

There are two equations known as Born stability criteria for a cubic system is used to evaluate mechanical stability of materials as follows [15]:

$$(C_{11} - C_{12}) > 0, C_{11} > 0, C_{44} > 0, (C_{11} + 2C_{12}) > 0. \quad (5)$$

Bulk modulus is also restricted as

$$C_{12} < B < C_{11}. \quad (6)$$

Based on Eqs. (5) and (6), it can be predicted that  $\text{LiBH}_4$  and  $\text{Li}(\text{BH})_3$  are mechanically stable materials, since both materials obey the Born stability criteria. It is said that the elastic constants can give information about the materials strength such as  $C_{11}$  which indicates unidirectional compression (along the  $x$ -axis) [16]. Based on the elastic constant values on Table 1, it can be predicted that both materials will show greater resistance against unidirectional compression than shear deformation, since  $C_{11}$  values are higher than  $C_{44}$  values for both materials. Moreover,  $C_{11}$  is lower for  $\text{LiBH}_4$

**Table 2** The calculated Bulk modulus ( $B$ , GPa), Shear modulus  $G$  (GPa),  $G/B$  and  $B/G$  ratios, Poisson's ratios ( $\sigma$ ), and Young's modulus  $E$  (GPa) of  $\text{LiBH}_4$  and  $\text{Li}(\text{BH})_3$ 

Material	$B$	$G$	$G/B$	$B/G$	$\sigma$	$E$
$\text{LiBH}_4$	30.83	18.24	0.59	1.69	0.25	45.64
$\text{Li}(\text{BH})_3$	24.43	18.47	0.75	1.32	0.20	44.25

than that of  $\text{Li}(\text{BH})_3$ , exhibiting that  $\text{LiBH}_4$  will show weaker resistance against unidirectional compression than  $\text{Li}(\text{BH})_3$  [17].

The obtained elastic constants are then used to drive several parameters which enable to understand fundamental and mechanical strength of the materials. The computed parameters are presented in Table 2. The details of computations can be found in [17]. The first parameter that is calculated is bulk modulus which describes materials response to a shape change under an external pressure. Therefore, this value can be used to predict average bond strength because of atoms' binding or cohesive energies. Higher bulk modulus indicates higher resistance towards shape change [18].  $\text{LiBH}_4$  has greater bulk modulus than  $\text{Li}(\text{BH})_3$  as given in Table 2, and thus,  $\text{LiBH}_4$  will display higher resistance towards shape change compared to  $\text{Li}(\text{BH})_3$ . Shear modulus,  $G$ , is defined as the ratio of shear stress and strain. The larger value of shear modulus means more directional bonding between atoms. Shear modulus of both materials is similar to each other, showing that both materials will give similar response to shear deformation.

The ratio between bulk modulus and shear modulus was proposed by Pugh [19]. According to Pugh's criteria, it is possible to predict the materials' ductile or brittle behaviour. The material is regarded as ductile if  $B/G$  ratio is above 1.75, and the material is regarded as brittle if  $B/G$  ratio is below 1.75. Based on that, it can be said that both  $\text{LiBH}_4$  and  $\text{Li}(\text{BH})_3$  are brittle materials which means that an extra caution is required when handling or transporting the materials. In addition, Cauchy pressure,  $C_p$ , can be used to estimate brittleness and angular characteristics of materials. If  $C_p$  is negative that implies brittle behaviour along with directional bonding with angular character, if  $C_p$  is positive that indicates ductile behaviour and metallic nature [20–22]. The calculated Cauchy pressures of both materials are negative which indicates brittleness of the materials. That result is in accordance with  $B/G$  ratio.

Another critical parameter that is computed is Poisson's ratio. This ratio is an indication of crystal stability against shear. Greater Poisson's ratio means better plasticity [23, 24]. In the case of  $\sim 0.1$  value of  $\sigma$ , the material will have dominant covalent characteristics, if is  $\sim 0.25$  value the material will have dominant ionic characteristics [25]. In addition, it was said that 0.5 and 0.25 are upper and lower limits for  $\sigma$  ratio for central force of a solid [16]. Both materials have their Poisson's ratios around 0.25 which implies both have dominant ionic characteristics.

**Table 3** The calculated Cauchy pressures ( $C_p$ , GPa), Vickers hardness ( $H_v$ , GPa), anisotropy factor ( $A$ ), and Melting temperatures ( $T_m$ , K) of  $\text{LiBH}_4$  and  $\text{Li}(\text{BH})_3$ 

Material	$C_p$ ( $C_{12}-C_{44}$ )	$H_v^G$	$H_v^E$	$A$	$T_m$
$\text{LiBH}_4$	- 2.63	0.327	2.774	2.53	817.47
$\text{Li}(\text{BH})_3$	- 6.71	0.368	2.690	0.73	872.73

Young Modulus ( $E$ ) describes the ratio of tensile stress to tensile strain. The stiffness of materials increase with Young modulus [26]. As Table 2 displays  $\text{LiBH}_4$  and  $\text{Li}(\text{BH})_3$  have similar values of Young modulus, meaning that both materials have similar stiffness.

The anisotropy factor, Vickers hardness, and melting temperatures of  $\text{LiBH}_4$  and  $\text{Li}(\text{BH})_3$  are also obtained and presented in Table 3. The anisotropy of materials affects the physical properties such as microcracks due to anisotropic thermal expansion coefficients in different planes and elastic anisotropy. It is especially critical for high technology applications, since it allows to predict the durability of the material and to measure intensity of the material in different directions [27, 28]. Therefore, the anisotropy of both materials is calculated using the elastic constants ( $A = 2C_{44}/C_{11}-C_{12}$ ) and given in Table 3. The unity in  $A$  value indicates isotropic material and any deviation from the unity implies anisotropy. Based on the data in Table 3, both  $\text{LiBH}_4$  and  $\text{Li}(\text{BH})_3$  are anisotropic materials, whereas  $\text{LiBH}_4$  shows greater anisotropy compared to  $\text{Li}(\text{BH})_3$ .

The calculation of elastic constants enables one to predict some macroscopic properties such as Vickers hardness. After calculation of Shear and Young modulus, these parameters are used to compute Vickers hardness given in [29]. It is suggested that materials with hardness greater than 10 GPa can be classified as hard material [30]. Based on the results of Vickers hardness, it is seen that both  $\text{LiBH}_4$  and  $\text{Li}(\text{BH})_3$  cannot be classified as hard materials, since both materials harnesses are found less than 10 GPa. The other significant property that can be calculated by using elastic constant is melting temperature. Melting temperatures of materials are important especially for industrial applications. For a cubic structure, the melting temperature can be obtained using the  $T_m = 553 + 5.91C_{11}$  relation [29]. Melting temperature of  $\text{LiBH}_4$  is computed as 817.47 K and 872.73 K for  $\text{Li}(\text{BH})_3$ .

The pressure dependence of lattice parameter (Fig. 3a), elastic constants (Fig. 3b), bulk (Fig. 3c), Shear (Fig. 3d), and Young modulus (Fig. 3e) of  $\text{LiBH}_4$  and  $\text{Li}(\text{BH})_3$  was also studied within 0–200 kbar range and presented in Fig. 3. Bulk modulus, and Young and shear modulus of both materials tend to increase with the increasing pressure, showing that stiffness, resistance towards shape change and deformation of the materials.  $C_{11}$  value of materials exhibit greater increase with the pressure compared to other elastic constants.  $C_{11}$  represents unidirectional compression along the  $x$ -axis which seem to increase with pressure

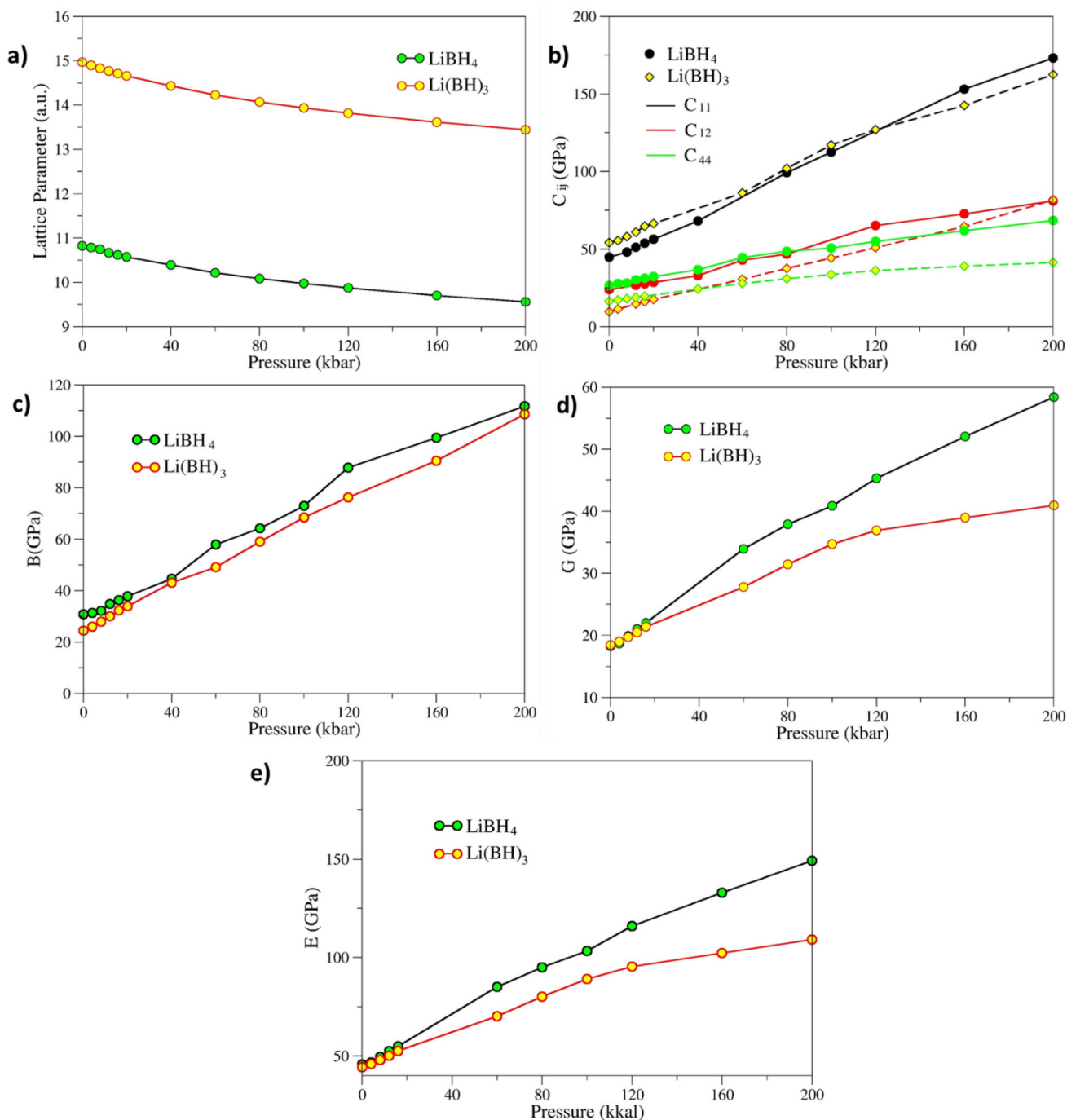


**Fig. 3** The pressure dependence of lattice parameter (a), elastic constants (b), bulk (c), shear (d), and Young modulus (e) of LiBH<sub>4</sub> and Li(BH)<sub>3</sub>

for both materials. In general,  $C_{11}$  means elasticity in height when a change is produced by a longitudinal strain. In this case, elasticity in height here for both materials is greater than elasticity in shape.

### 3.2 Electronic properties

The calculated electronic band structures of LiBH<sub>4</sub> and Li(BH)<sub>3</sub> which crystallize in the cubic phase with the

space groups  $F\bar{4}3m$  (Fig. 4a) and  $Fm\bar{3}m$  (Fig. 4b), respectively, along with the high symmetry directions are given in Fig. 4. Fermi energy level is set to 0 eV. As Fig. 4 illustrates that both of LiBH<sub>4</sub> and Li(BH)<sub>3</sub> exhibit non-metallic behaviour, since there are band gaps around the Fermi level as 6 eV and 4.58 eV, respectively. As Fig. 5a displays for LiBH<sub>4</sub>, from  $-8$  to  $-5.5$  eV B 2p and H 1s states dominate and from 1.5 to 6 eV is dominated by Li 2s, Li 2p and H 1s states.

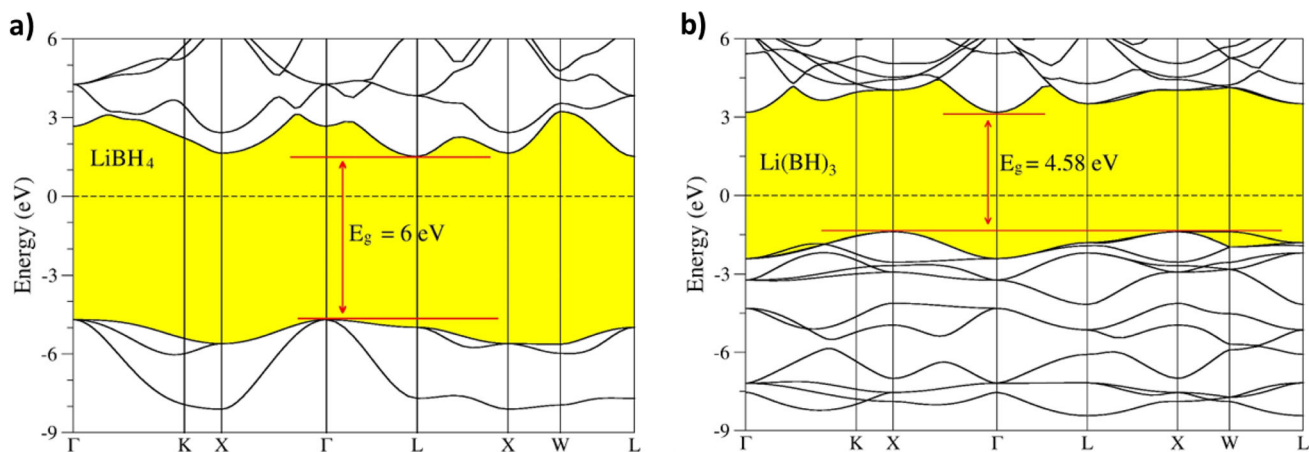


**Fig. 4** The calculated electronic band structures of  $\text{LiBH}_4$  and  $\text{Li}(\text{BH})_3$

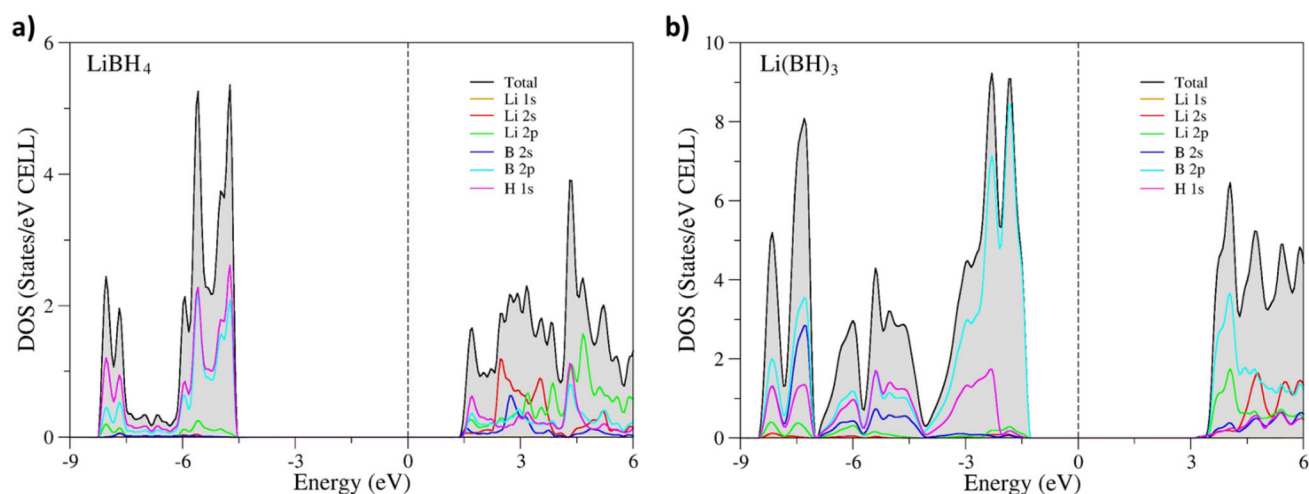


**Fig. 5** The partial and total DOS of  $\text{LiBH}_4$  and  $\text{Li}(\text{BH})_3$

For  $\text{Li}(\text{BH})_3$  in Fig. 5b, B 2p, B 2ps, and H 1s states contribute to valance band, whereas Li 2p, Li 2s, and B 2p states contribute to the conduction band.

### 3.3 Hydrogen storage properties

$\text{LiBH}_4$  and  $\text{Li}(\text{BH})_3$  crystallize in the cubic phase with the space groups  $F\bar{4}3m$  and  $Fm\bar{3}m$  and they are found to be mechanically stable. To use  $\text{LiBH}_4$  and  $\text{Li}(\text{BH})_3$  as hydrogen storage materials, some of hydrogen storage properties are also calculated. Gravimetric hydrogen density (GHD) is a critical feature for solid-state hydrogen storage. GHD of  $\text{LiBH}_4$  and  $\text{Li}(\text{BH})_3$  is obtained via the equation below [31]

$$C_{\text{wt}\%} = \left( \frac{(H/M)M_H}{M_{\text{Host}} + (H/M)M_H} \times 100 \right) \%, \quad (7)$$

where  $H/M$  is hydrogen-to-metal ratio,  $M_H$  is molar mass of hydrogen, and  $M_{\text{Host}}$  is molar weight of host material. Based on this computation, GHD of  $\text{LiBH}_4$  is obtained as 15.61 wt% and for  $\text{Li}(\text{BH})_3$  is obtained

as 6.65 wt% which are higher rate than that is set by US Energy Department which is 4.5 wt% for practical applications [32].

Another critical feature that needs to be computed for hydrogen storage is that hydrogen desorption temperature which determines the temperature required for hydrogen release from the material. Hydrogen desorption temperature can be computed from formation enthalpy of the material and entropy change of hydrogen which is given as 130.7 J/mol K [33]. The relation is given as

$$\Delta H = T_d \times \Delta S, \quad (8)$$

where  $T_d$  represents hydrogen desorption temperature. Using Eq. (4), desorption temperature for  $\text{LiBH}_4$  is calculated as about 198.2 K and for  $\text{Li}(\text{BH})_3$  is about 138.6 K.

## 4 Conclusions

Several properties of cubic  $\text{LiBH}_4$  and  $\text{Li}(\text{BH})_3$  have been investigated by means of first principles calculations. The formation energies of both materials showed that materials are synthesisable.  $\text{LiBH}_4$  and  $\text{Li}(\text{BH})_3$  are mechanically stable based on the evaluation of their elastic constants. Both materials have their Poisson's ratios around 0.25 which implies that both have dominant ionic characteristics. Cauchy pressures and  $B/G$  ratio indicate brittle nature for both of them. The anisotropy factor suggests that both materials show anisotropic behaviour. The electronic band structures exhibit band gaps around Fermi level, suggesting that both materials are non-metallic. The gravimetric hydrogen density is computed as 15.61 wt% for  $\text{LiBH}_4$  and 6.65 wt% for  $\text{Li}(\text{BH})_3$ . Also, the hydrogen desorption temperature for  $\text{LiBH}_4$  is calculated as about 198.2 K and for  $\text{Li}(\text{BH})_3$  is about 138.6 K.

**Acknowledgements** Not applicable.

## Author contributions

All authors have contributed equally to the preparation of the manuscript.

**Funding** There is no funding received for this study.

**Data availability** The data are available from the corresponding author on reasonable request.

## Declarations

**Conflict of interest** The authors declare no competing interests.

## References

- M. Hermesmann, T.E. Müller, Prog. Energy Combust. Sci. **90**, 100996 (2022)
- A. Tekin, R. Caputo, A. Züttel, Phys. Rev. Lett. **104**(21), 215501 (2010)
- S. Li, X. Ju, C. Wan, Comput. Mater. Sci. **81**, 378–385 (2014)
- R.M.A. Khalil, M.I. Hussain, F. Hussain, A.M. Rana, G. Murtaza, M. Shakeel, H.M. Asif Javed, Int. J. Quantum Chem. **121**(4), e26444 (2021)
- Y. Bouhadda, S. Djellab, M. Bououdina, N. Fenineche, Y. Boudouma, J. Alloys Compd. **534**, 20–24 (2012)
- H. Benzidi, M. Garara, M. Lakhali, M. Abdalaoui, A. Benyoussef, A. Elkenz, M. Louilidi, M. Hamedoun, O. Mounkachi, Int. J. Hydrogen Energy **43**(13), 6625–6631 (2018)
- X.B. Yu, D.M. Grant, G.S. Walker, J. Phys. Chem. C **113**(41), 17945–17949 (2009)
- X. B. Yu, Z. Wu, Q. R. Chen, Z. L. Li, B. C. Weng and T. S. Huang, Appl. Phys. Lett. **90**(3) (2007).
- P. Giannozzi, S. Baroni, N. Bonini, M. Calandra, R. Car, C. Cavazzoni, D. Ceresoli, G.L. Chiarotti, M. Cococcioni, I. Dabo, J. Phys. Condens. Matter **21**(39), 395502 (2009)
- J.P. Perdew, K. Burke, M. Ernzerhof, J Phys. Rev. Lett. **77**(18), 3865 (1996)
- M. Methfessel, A. Paxton, J. Phys. Rev. B **40**(6), 3616 (1989)
- M.I. Hussain, R.M. Arif Khalil, F. Hussain, A.M. Rana, G. Murtaza, M. Imran, Optik **219**, 165027 (2020)
- M.I. Hussain, R.M.A. Khalil, Mater. Sci. Semicond. Process. **152**, 107050 (2022)
- M.I. Hussain, R.M.A. Khalil, F. Hussain, **9**(5), 2001026 (2021).
- A.H. Reshak, M.Y. Shalaginov, Y. Saeed, I.V. Kityk, S. Auluck, J. Phys. Chem. B **115**(12), 2836–2841 (2011)
- S. Benlamari, H. Bendjeddou, R. Boulechfar, S. Amara Korba, H. Meradji, R. Ahmed, S. Ghemid, R. Khenata, S. Bin Omran, Chin. Phys. B **27**(3), 037104 (2018)
- S. Al, Int. J. Hydrogen Energy **44**(3), 1727–1734 (2019)
- P. Li, J. Zhang, S. Ma, Y. Zhang, H. Jin, S. Mao, MoSim **45**(9), 752–758 (2019)
- S.F. Pugh, Philos. Mag. J. Sci. **45**(367), 823–843 (1954)
- H. Ziani, A. Gueddim, N. Bouarissa, L. Gacem, Mater. Sci. Eng. B **269**, 115154 (2021)
- H. Ziani, A. Gueddim, N. Bouarissa, J. Mol. Model. **29**(2), 59 (2023)
- N. Miao, B. Sa, J. Zhou, Z. Sun, Comput. Mater. Sci. **50**(4), 1559–1566 (2011)
- L. Liu, X. Wu, R. Wang, X. Nie, Y. He, X. Zou, Crystals **7**(4), 111 (2017)
- A. Gueddim, S. Zerroug, N. Bouarissa, N. Fakroun, ChJPh **55**(4), 1423–1431 (2017)
- V.V. Bannikov, I.R. Shein, A.L. Ivanovskii, Phys. Status Solidi (RRL) Rapid Res. Lett. **1**(3), 89–91 (2007)
- A. Gencer, G. Surucu, S. Al, Int. J. Hydrogen Energy **44**(23), 11930–11938 (2019)
- S. Al, in *Zeitschrift für Naturforschung A*, Vol. 74, (2019), p. 1023.
- N. Miao, B. Sa, J. Zhou, Z. Sun, presented at the Computational Materials Science (2011) (**Unpublished**).
- H. Chen, L. Yang, J. Long, Superlattices Microstruct. **79**, 156–165 (2015)
- T. Özer, J. Can. J. Phys. **98**(4), 357–363 (2020)
- D.P. Broom, *Hydrogen Storage Materials; The Characterisation of Their Storage Properties*, 1st edn. (Springer, London, 2011)
- D. Pukazhselvan, V. Kumar, S.K. Singh, Nano Energy **1**(4), 566–589 (2012)
- Q. Zeng, K. Su, L. Zhang, Y. Xu, L. Cheng, X. Yan, J. Phys. Chem. Ref. Data **35**(3), 1385–1390 (2006)

Springer Nature or its licensor (e.g. a society or other partner) holds exclusive rights to this article under a publishing agreement with the author(s) or other rightsholder(s); author self-archiving of the accepted manuscript version of this article is solely governed by the terms of such publishing agreement and applicable law.